energy&fuels

Article

pubs.acs.org/EF

Experimental Investigation of Spark-Ignited Combustion with High-Octane Biofuels and EGR. 2. Fuel and EGR Effects on Knock-Limited Load and Speed

Derek A. Splitter* and James P. Szybist†

Fuels, Engines, and Emissions Research Center, Oak Ridge National Laboratory, NTRC Building, 2360 Cherahala Blvd, Knoxville, Tennessee 37932, United States

ABSTRACT: The present study experimentally investigates spark-ignited combustion with 87 AKI E0 gasoline in its neat form and in midlevel alcohol−gasoline blends with 24% vol/vol isobutanol−gasoline (IB24) and 30% vol/vol ethanol−gasoline (E30). A single-cylinder research engine is used with an 11.85:1 compression ratio, hydraulically actuated valves, laboratory intake air, and was capable of external exhaust gas recirculation (EGR). Experiments were conducted with all fuels to full-load conditions with $\lambda = 1$, using both 0% and 15% external-cooled EGR. Higher octane number biofuel blends exhibited increased stoichiometric torque capability at this compression ratio, where the unique properties of ethanol enabled a doubling of the stoichiometric torque capability with E30 as compared to that of 87AKI, up to 20 bar IMEPg (indicating mean effective pressure gross) at $\lambda = 1$. The results demonstrate that for all fuels, EGR is a key enabler for increasing engine efficiency but is less useful for knock mitigation with E30 than for 87AKI gasoline or IB24. Under knocking conditions, 15% EGR is found to offer 1°CA of CA50 timing advance with E30, whereas up to 5°CA of CA50 advance is possible with knock-limited 87AKI gasoline. Compared to 87AKI, both E30 and IB24 are found to have reduced adiabatic flame temperature and shorter combustion durations, which reduce knocking propensity beyond that indicated by the octane number. However, E30+0% EGR is found to exhibit the better antiknock properties than either 87AKI+15% EGR or IB24+15% EGR, expanding the knock limited operating range and engine stoichiometric torque capability at high compression ratio. Furthermore, the fuel sensitivity (S) of E30 was attributed to reduced speed sensitivity of E30, expanding the low-speed stoichiometric torque capability at high compression ratio. The results illustrate that intermediate alcohol−gasoline blends exhibit exceptional antiknock properties and performance beyond that indicated by the octane number tests, particularly E30.

INTRODUCTION

The Energy Independence and Security Act[1] of 2007 requires that by year 2022, 36 billion gallons per year of bioderived fuels need to be consumed in transportation. This uptake in bioderived fuels is a more than a 7-fold increase from the 4.7 billion gallons consumed per year when the law was enacted. The rules for complying with this mandate are specified by the US Environmental Protection Agency (EPA) in the Renewable Fuel Standard II (RFS II).[2] When the total transportation energy consumption is analyzed, it is apparent that this legislation increases the usage of biofuels. In 2012, the United States consumed 27.97 quadrillion BTU of energy for transportation and is projected to consume 29.24 quadrillion BTU in 2022.[3] Assuming a gasoline equivalent energy of 42.8 MJ/kg and density of 740 kg/m,[3] the RFS II standard will require an increase in the percentage of transportation energy from biofuels to approximately 14% in 2022 from the approximate 2% in 2007. To date, the RFS II progress has seen more than a doubling of biofuel usage, with the annual recorded share of transportation energy from nonpetroleum sources totaling 4.3% in 2012. Although 2012 was the year with the largest biofuel energy share on record,[3] there is still an additional 3-fold increase in biofuel energy share required to comply with the RFS II mandate.

Concurrent with RFS II, legislation by the National Highway and Transportation Safety Administration passed in 2011 requires an effective 2-fold increase in corporate average fuel economy (CAFE) standards to achieve 54.5 US miles per gallon by 2025,[4] an effective 2-fold increase compared with present CAFE standards. Ideally, The RFS II and CAFE mandates could be met simultaneously through proper exploration and implementation of high-efficiency biofuel engines.

In the United States, the stoichiometrically operated spark ignition (SI) engine has maintained over a 99% market share in the light-duty (LD) vehicle sector (passenger cars and pickup trucks) since 1985,[5] and over a 94% share since the EPA began record keeping in 1975. This LD sector engine dominance is due primarily to the facts that the SI engine has low production cost, low fuel cost, rugged operation, high power and torque density, low sooting tendency, and can employ known mature catalyst technologies to reduce regulated emissions (nitric oxide (NO_x), hydrocarbon (HC), and carbon monoxide (CO)). The market sector dominance with the SI engine in combination of legislated CAFE and RFS II standards suggests that increases to SI engine efficiency with biofuels might offer a very plausible path toward simultaneous CAFE and RFS II compliance.

Although the SI engine has many beneficial attributes, its efficiency is fundamentally hindered by the throttling of air, and its compression ratio is limited by combustion knock. These two factors result in lower thermal efficiency (defined as the efficiency of converting fuel chemical energy to mechanical output work) of

Received: August 7, 2013
Revised: December 21, 2013

   dx.doi.org/10.1021/ef401575e | *Energy Fuels* XXXX, XXX, XXX−XXX

SI engines relative to compression-ignited engines (i.e., diesel engines) or lean-burn SI engines. Historically, engine improvements have focused primarily on increasing power, safety, and convenience, yielding increases in performance and vehicle weight, while complying with regular legislated fuel economy mandates, which have been near constant since 1985.[5] The progress in engine performance over the years can clearly be observed when viewed relative to a 1975 baseline (the first year of EPA records): in today's vehicles, the industry average power-per-unit displacement has more than doubled, whereas vehicle zero to 60 miles per hour acceleration time has halved.[5] This evolutionary increase in performance has resulted in a 50% reduction in the average modern light-duty engine displacement compared with a 1975 era engine. Although these trends show there has been significant progress in engine performance, to comply with future CAFE requirements, engine and vehicle efficiency must also be addressed and improved.

An evolutionary strategy for achieving CAFE compliance while retaining performance is downsizing and turbocharging with direct injection. These two technologies offer increased engine power and torque density with equal or similar performance when downsizing and downspeeding of engines, a proven efficiency-improving strategy.[6] However, the opportunity for downsizing and downspeeding becomes limited by combustion knock from the octane number and physical−chemical properties of current market available fuels, thereby limiting thermodynamic efficiency.

Unlike distillate fuels, alcohol fuels exhibit some key properties that make them particularly attractive fuels for future engines. Most notably, alcohol fuels tend to have a high octane number and lower carbon intensity (defined as the number of moles of carbon per unit of energy (LHV)). These combinations of properties grant alcohol-based fuels a 2-fold reduction potential in tailpipe carbon dioxide (CO_2) through molecular advantage and the ability to tolerate higher engine compression ratios. Additionally, alcohol fuels exhibit two other properties that can be favorable for increasing engine efficiency:

First, alcohol fuels exhibit a high latent heat of vaporization (HoV), which when used in conjunction with direct injection (DI) fueling, can increase the incoming charge density caused by a reduction in charge temperature. When exploited properly, the high HoV improves engine breathing as highlighted by Stein et al.[7] and mitigates combustion knock tendency. The effect of HoV has proved to be strong, even in a sparingly used dual-fuel arrangement, where the charge cooling of a small amount of direct-injected ethanol prevented knock and extended the torque capability,[8] with both benefits enabling higher-efficiency engines.

Second, the amount of thermodynamic work that can be extracted from ethanol on a second-law basis is higher than is suggested by its lower heating value (LHV) alone (i.e., exergy and LHV). This is attributed to a high yield of molar products for alcohols on both a stoichiometric and energy basis relative to petroleum distillates, increasing expansion pressure.[9,10] Ford and AVL have shown that ethanol enables efficiency improvements, with several notable works summarized in Stein et al.[11] Vehicle-specific effects were researched by Jung et al.[12] at light load conditions and also in an additional study by Jung et al.[13] with drive cycle and engine efficiency estimates. The latter study points out that a light-duty pickup truck engine with intermediate ethanol−gasoline blends could be optimized such that the thermal efficiency increase with ethanol−gasoline blends of 20% ethanol vol/vol are sufficiently high to at least offset the fuel mileage penalty of alcohol fuels (miles per gallon, MPG) and achieve even greater tailpipe CO_2 reductions.

These engine experiment and vehicle simulation results demonstrate that reductions in CO_2 emissions without a decrease in MPG could be possible with intermediate ethanol−gasoline blends. A major reason for this prediction is the ability of ethanol addition to reduce combustion knock and enable an increased compression ratio. Interestingly, work by Szybist and West[14] demonstrates that blending ethanol, even with very low-octane gasoline blendstocks, offers significant antiknock resistance and that a high-octane fuel can be produced through blending intermediate levels of ethanol with straight-run gasoline. This is because of the highly nonlinear response of octane number blending with ethanol on a volumetric basis, as previously explained in detail by Anderson et al.[15,16] and more recently by Foong et al.[17] These cited studies show that intermediate-level ethanol blends might be promising for the next generation of SI engine fuels. The noted inherent benefits provide the potential to increase the power output and efficiency of the engine through fuel-based knock mitigation coupled to engine optimization. However, as pointed out in the 2013 SAE International High Octane Fuel Symposium,[18] multiple levels of cooperation from the fuel industry, legislation and regulatory bodies, distribution systems, and point of sale vendors is required if fuel octane number is to be increased.

The use of external cooled exhaust gas recirculation (EGR) could be a more direct approach to increasing SI engine efficiency. External EGR is a proven method to reduce the knocking tendency for a given fuel. External-cooled EGR has been employed for years in diesel engines, with recent interest gaining in SI engines. The constituents of EGR in SI engines differ from those in their diesel counterparts. Specifically, $\lambda = 1$ SI EGR is oxygen deficient, meaning that SI EGR offers the potential to increase charge mass without changing the oxygen content. The lack of oxygen in SI EGR is important when considering both catalyst and throttling requirements of SI engines (i.e., $\lambda = 1$). In addition to reducing throttling losses, the introduction of EGR into SI engines improves the thermodynamic properties of the working fluid (i.e., the ratio of specific heats [γ]), reducing in-cylinder temperatures and improving knock resistance.

Many of these thermodynamic advantages have been documented by others. For example, Alger et al.[19] showed that external-cooled EGR effectively decreased the knocking propensity of distillate fuel, which functionally increased the fuel octane number. However, EGR also slowed the flame kernel growth because of slowed reaction rates. Therefore, higher EGR levels in SI engines might require the incorporation of different higher turbulence combustion chamber flows to increase EGR tolerance, as shown by Wheeler at al.,[20] or through high-energy long spark systems, as shown by Alger et al.[21] These previous studies suggest that there are technical challenges that need to be addressed for implementation with current market fuels if EGR is to be used.

The relation between knock mitigation and cycle difference with external-cooled EGR raises several questions:

1. Can knock resistance of conventional distillate fuels be sufficiently improved to the levels of midlevel alcohol blends through the addition of EGR?
2. What, if any, role does EGR have on engine efficiency in midlevel alcohol blends?

dx.doi.org/10.1021/ef401575e | Energy Fuels XXXX, XXX, XXX−XXX

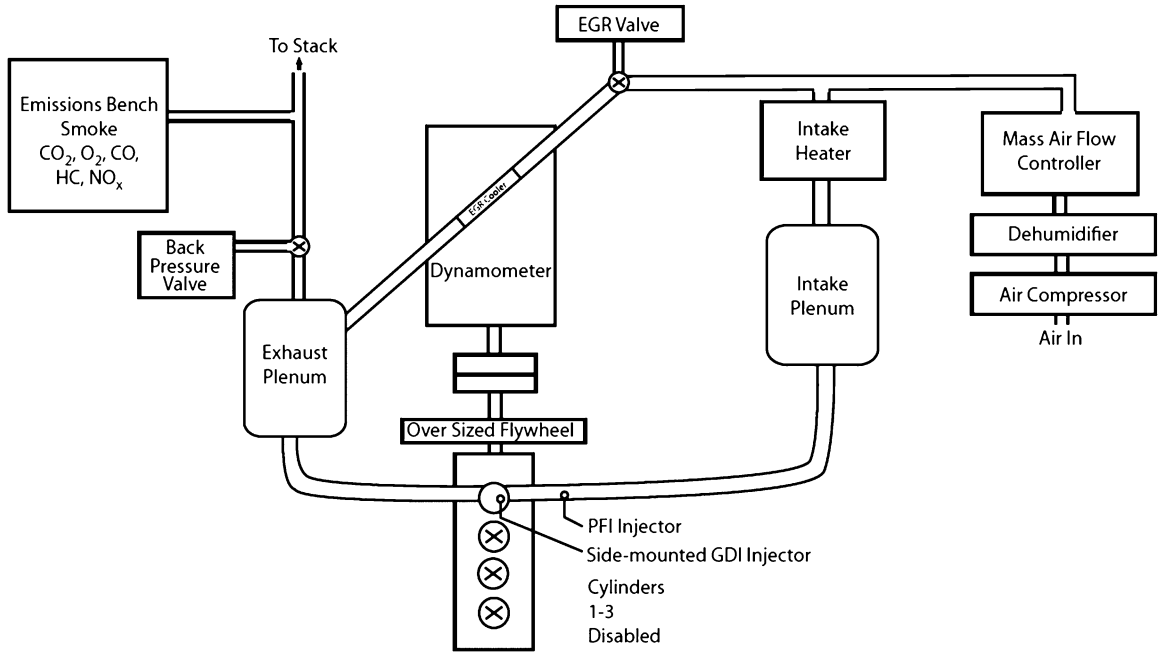

Figure 1. Schematic of the experimental configuration.

3. What are the combustion-specific differences between intermediate alcohol−gasoline blends and neat gasoline?
4. What, if any, potential performance and fuel economy incentives do midlevel alcohol−gasoline fuel blends offer, both with and without external-cooled EGR?
5. Can intermediate alcohol−gasoline fuel blends enable new powertrain possibilities?

This study is partitioned into two separate manuscripts. Both parts explore the use of midlevel ethanol and isobutanol gasoline blends compared with conventional gasoline, each with 0% and 15% external-cooled EGR. The current results (part 2 of 2) explore the differences in combustion and efficiency between each fuel using a detailed combustion analysis and thermodynamic approach. The antiknock phenomena are explored on a load, phasing, and speed basis. The results complement the companion paper (part 1),[32] which explores engine efficiency, stoichiometric torque capability at high compression ratio, and downsizing + downspeeding potential of each fuel−EGR combination relative to one another, with E30+15% EGR also compared with high-efficiency conventional diesel engine data.

EXPERIMENTAL DETAILS

This study explores SI engine operation at five engine speeds (1200, 1600, 2000, 2500, and 3000 r/min) and two different EGR rates (0% and 15%), each with three different fuels (87AKI E0 "regular" gasoline, 30% by vol ethanol−gasoline, and 24% by vol isobutanol−gasoline). A highly modified 2.0 L GM Ecotec SI engine with stock side mounted direct fuel injector is used. Three cylinders of the production engine are disabled to allow single-cylinder operation with an installed custom-domed piston, which increases the compression ratio to 11.85:1 (stock 9.2:1). Notably, the increase in compression ratio changes many attributes of the combustion chamber geometry, therefore complicating a direct comparison of the higher compression ratio data to the stock compression ratio. Splitter and Szybist[22] discuss observed differences in combustion and emissions between the stock 9.2 and modified 11.85 compression ratio pistons, but the current study omits the direct comparison.

The SI engine is operated with a laboratory air-handling system. Pressurized and dried facility air that has less than 5% relative humidity is metered to the engine using a mass air-flow controller. The present study omits humidity effects, where added humidity may have an effect of reducing knock. The engine is equipped with separate electromechanical valves for backpressure and external EGR, enabling the capability for independent control of intake manifold pressure, exhaust manifold pressure, and EGR. Cooled EGR mixes with fresh air upstream from an air heater, followed by the intake plenum, and then the intake manifold. EGR is measured using an EGR 5230 system from ECM, an instrument that uses pressure-compensated wideband oxygen sensors in both the intake and exhaust to nonintrusively measure EGR. When EGR was used, a constant rate of 15 ± 1% was supplied. A schematic of the laboratory is provided in Figure 1.

The engine is equipped with a hydraulic valve actuation (HVA) system to enable fully variable valve actuation. To accommodate the small research module HVA system from Sturman Industries, the cylinder head has been machined, disabling the functionality of the production cam and fuel pump systems. Details of the HVA system have been published previously.[9,14,23] The engine geometry is listed in Table 1.

Table 1. Engine Geometry

bore × stroke	86 × 86 mm
connecting rod length	145.5 mm
compression ratio	11.85:1
fuel injection system	direct injection, side-mounted

Crank-angle (CA) resolved data are recorded at 1800 samples per revolution (0.2°CA resolution) for 300 consecutive cycles. Cylinder pressure is measured using a Kistler piezoelectric 6125B pressure transducer coupled to a Kistler 5010 charge amplifier. Additionally, the DI command signal and intake and exhaust valve lift from each of the four HVA valves is recorded on a crank-angle resolved basis. All indicated results presented in this study are for a 300 cycle average.

Engine emissions are measured using a standard emissions bench with instruments manufactured by California Analytical Instruments. NO_x emissions are measured using a chemiluminescence analyzer, CO and CO_2 are measured using infrared analyzers, oxygen (O_2) is measured using a paramagnetic analyzer, and unburned HC are measured with a flame ionization detector. Smoke measurements are performed using an AVL 415s filter smoke number instrument. To measure the fuel flow rate (and thus efficiency), the air-to-fuel ratio

dx.doi.org/10.1021/ef401575e | *Energy Fuels* XXXX, XXX, XXX−XXX

(AFR) is measured directly from a Coriolis-effect fuel flow meter and a laminar air flow element. The corresponding fuel flow is then cross-referenced to independently calculate air-to-fuel ratios from the engine exhaust using both the emissions bench and automotive wideband oxygen sensor approaches.

The conditions maintained for all fuels, engine speeds, loads, and EGR combinations are listed in Table 2.

Table 2. Constant Operating Conditions

exhaust valve open at 0.8 mm lift (°CA ATDC$_f$)	170
exhaust valve close at 0.8 mm lift (°CA ATDC$_f$)	350
max exhaust valve lift (mm)	9
intake valve open at 0.8 mm lift (°CA ATDC$_f$)	−355
intake valve close at 0.8 mm lift (°CA ATDC$_f$)	−170
max intake valve lift (mm)	9
start of DI command (°CA ATDC$_f$)	−280
intake manifold gas temperature (°C)	52
engine coolant (°C)	90
oil (°C)	90
exhaust λ (-)	1
DI rail pressure (bar)	100

Five engine speeds of 1200, 1600, 2000, 2500, and 3000 r/min were tested with gross load increments (IMEPg, indicating mean effective pressure gross) of 50 ± 5 kPa. The constraints and load range for E30 without EGR are seen in Figure 2, which illustrates the tested operational map up to the constraints for E30 with 0% EGR. The identical procedure and setup is conducted for each fuel type and both EGR rates.

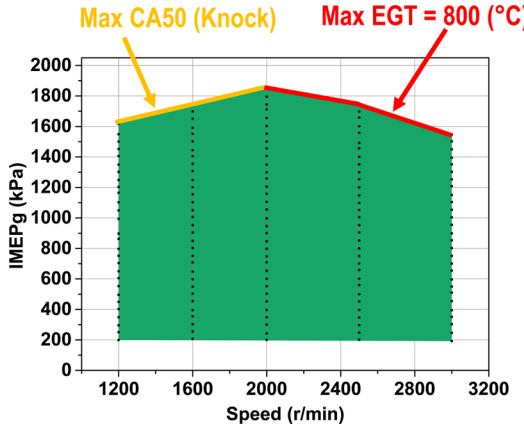

Figure 2. Representative engine load-speed range tested with knock and EGT constraints indicated.

All fuels and EGR rates are tested at maximum brake torque (MBT) timing until combustion knock is encountered. Once knock-limited, combustion is phased through spark timing to maintain a constant level of knock through visual inspection of the indicated pressure trace and by maintaining constant AVL combustion noise. The tested load range is from 2 bar IMEPg to full load, which is defined as the maximum load without enrichment (λ = 1) with limits on CA50 (crank angle at 50% mass fraction burned) combustion phasing of 25°CA ATDC$_f$, peak cylinder pressure of 10 000 kPa, and exhaust gas temperature (EGT) of 800 °C. (Note that CA50 combustion phasing later than 25°CA ATDC$_f$ is not ideal for high efficiency, which is the focus of the present study. Additionally, 800 °C EGT limit is imposed because, unlike the production engine, the Sturman valvetrain does not use sodium-filled values, which can withstand higher exhaust gas temperatures. The maximum cylinder pressure limit is set because the stock engine is rated to 10 000 kPa, although this constraint is not reached by any of the present fuel or experimental condition combinations.) Figure 2 displays the constraint limits reached with 0% EGR E30 operation.

The only exception to the constraints is at the lightest loads with EGR (IMEPg ≤ 250 kPa), where combustion is unstable at MBT CA50 phasing, where later than MBT CA50 were found to improve stability. The constraint used to bound the amount of CA50 retard for acceptable operation at these lightest loads is CA50 ≤ 15°CA ATDC$_f$. Using these limits, operation with each fuel is compared.

The production spark plug heat range and gap is used for all tests. However, the spark energy is generated with an aftermarket MSD DIS6-2 Plus multistrike ignition system to increase the combustion stability at high EGR levels. The MSD system is capable of up to three consecutive spark discharges per cycle, but the number of discharges is speed dependent, with only one or two discharges at higher engine speeds. The spark coil signal from the MSD system, heat release rate (HRR), and cylinder pressure are indicated in Figure 3, along with the

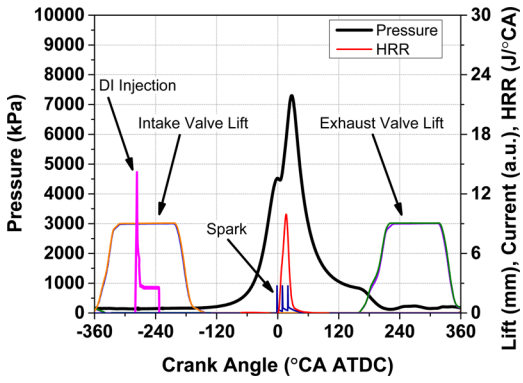

Figure 3. Representative high-load fired case showing indicated cylinder pressure and apparent HRR with corresponding valve, spark, and injection event schedule.

unique valve events provided by the Sturman HVA system. The near square valve lift profile generated by the Sturman HVA system differs from conventional valve lift and duration dynamics, resulting in increased flow area with different engine breathing and charge motion characteristics. The specific differences between the HVA valvetrain and a cam-based valvetrain are discussed in a previous publication.[24]

When operating with higher-than-atmospheric pressures, a constant overall turbocharger efficiency of 25% with no intake or exhaust pressure restrictions is assumed (i.e., no muffler pipe, catalysis, or air cleaner pressure losses assumed). This assumption is considered valid and conservative because the production turbocharger for this SI engine is capable of over 55% combined overall efficiency. The combined turbocharger efficiency is calculated based on the air standard model as explained in Heywood[25] (eq 1) using intake and exhaust surge tank pressures and temperatures measured in the ports and assuming 100% turbine shaft mechanical efficiency. When operating with external EGR, the electromechanical valves for backpressure and EGR were modulated as needed to maintain 15% EGR and 25% combined turbocharger efficiency

Overall turbocharger efficiency calculation

$$\eta_{\text{combined}} = \frac{\left(\frac{\gamma_{\text{comp}}}{\gamma_{\text{comp}}-1}\right)\left(\frac{T_{\text{comp,in}}}{T_{\text{turb,in}}}\right)\left[\left(\frac{P_{\text{comp,in}}}{P_{\text{comp,out}}}\right)^{[(\gamma_{\text{comp}}-1)/\gamma_{\text{comp}}]}-1\right]}{\left(\frac{\gamma_{\text{turb}}}{\gamma_{\text{turb}}-1}\right)\left(1+\frac{1}{\text{AFR}}\right)\left[1-\left(\frac{P_{\text{turb,out}}}{P_{\text{turb,in}}}\right)^{[(\gamma_{\text{turb}}-1)/\gamma_{\text{turb}}]}\right]} \quad (1)$$

Fuels and Fuel Properties. Three fuels are tested; two fuels are alcohol−gasoline blends, and the third is an unblended gasoline. The two alcohol blended fuels were splash blended on site with either 24% neat isobutanol or 30% neat ethanol, with alcohol and gasoline volume fractions being measured in unblended fractions and then combined. All fuels were based on commercially obtained 87 AKI E0 "regular" pump fuel sourced directly from a distribution terminal. It should be

dx.doi.org/10.1021/ef401575e | Energy Fuels XXXX, XXX, XXX−XXX

noted that splash blending these alcohols with finished market E0 gasoline is not likely at an industrial scale if the tested blend ratios were to be market sold. More likely, a blendstock for oxygenate blends (BOB) fuel would be used, which tend to have lower octane numbers. Although using a BOB would decrease the research octane number (RON) of a blended fuel below those tested in the present study, other studies[7,14] have shown that the RON difference of a blended fuel based on a BOB vs a finished E0 is much smaller than the difference in RON between the unblended BOB and finished E0 fuels.

The blending ratios used are based on the following:

- The 24% isobutanol blend was selected as it has near identical oxygen content as E15, which the EPA has approved for use in 2001 and newer light duty vehicles.[26,27]
- The 30% ethanol blend was selected because, as the EPA recently stated,[28] there is no foreseeable issue with higher ethanol−gasoline blends; citing blends as high as E30 would likely be permissible.

These alcohol−gasoline-fuel-based fuels are of interest, as the neat alcohols used exhibit nearly identical motor octane number (MON) values and similar RON values.[29] However, the energy density of isobutanol is higher than that of ethanol on both a volume and mass basis, thus making its energy density closer to a gasoline. Additionally, the lower water solubility of isobutanol as compared to that of ethanol offers advantages in certain markets such as marine environments, where humidity and water contact are more likely. Interestingly, research by Stein et al.[11] has demonstrated that the Reid vapor pressure of intermediate ethanol blends are typically lower than E10 blends for the same blendstock, making such fuels attractive to regulatory bodies, as has been indicated in the recent EPA Tier III notification of proposed rulemaking.[28]

In the present study, the alcohols are from nondenatured reagent-grade purity and obtained directly from suppliers. Sigma-Aldrich supplied the isobutanol at a purity of >99%, and Decon Laboratories supplied the nondenatured ethanol. The three fuels were sent for independent analysis at an ASTM international-certified laboratory. The key chemical properties from the analysis are presented in Table 3, which shows that the fuels have significantly different chemical and physical properties.

Table 3. Fuel Properties

	87 AKI	IB24	E30
oxygenates ASTM D5599 (%v)	<0.1 any	23.64 isobutanol	30.65 ethanol
HoV (kJ/kg)[a]	352[29,30]	443[29,29,31]	529[29,29,31]
HoV with gasoline energy equiv (kJ/kg)[b]	352[29,30]	470[29−31]	599[29−31]
Reid vapor pressure, ASTM D5191 (psi)	13.13	12.29	13.28
10% distillation point, ASTM D86 (°C)	97	115	111
30% distillation point, ASTM D86 (°C)	144	175	150
50% distillation point, ASTM D86 (°C)	205	208	165
70% distillation point, ASTM D86 (°C)	253	222	170
90% distillation point, ASTM D86 (°C)	316	307	299
RON, ASTM D2699 (-)	90.2	96.6	100.3
MON, ASTM D2700 (-)	83.9	86.8	88.8
sensitivity (-)	6.3	9.8	11.5
LHV, ASTM D240 (MJ/kg)	43.454	40.846	38.105
λ = 1 AFR (-)	14.70	14.13	12.85
C, ASTM D5391 wt. (%)	86.49	80.63	74.4
H, ASTM D5391 wt. (%)	14.06	13.89	13.73
O, ASTM D5599 wt (%)	<0.1	3.71	11.34
specific gravity, ASTMD 4052 (-)	0.729	0.7423	0.745
volumetric energy density (MJ/gal)	119.5	114.5	107.1

[a]Calculated through a linear combination of neat alcohol and neat gasoline HoV. [b]Calculated on a gasoline equivalent energy basis (i.e., required for matched load).

RESULTS

Results are presented in five subsections. The first provides an overview of the engine speed and load range both with and without EGR. The second explores knock-limited combustion phasing for each fuel. The third discusses combustion duration differences between fuels. The fourth discusses sources of efficiency and losses and thermodynamic differences between the fuels. The fifth compares the fuels' knock-limited spark advance (KLSA) to engine speed and EGR.

Speed-Load Range Overview. Figure 4 presents the gross indicated load-speed range of the three fuels with and without EGR operated to the load limit constraints.

The results demonstrate that the higher octane fuels offer improved stoichiometric torque capability at high compression ratio, particularly with E30. With each fuel, EGR provides an additional benefit to extending the maximum load by enabling more advanced phasing at low engine speeds and reduced exhaust temperature at higher engine speed. An explanation for this is explored in greater detail throughout this manuscript. However, note that E30 effectively doubles the engine's stoichiometric torque capability at the tested compression ratio. A more detailed analysis and discussion of the performance effects of EGR is provided in the companion paper, part 1.[32]

Combustion Phasing Analysis. The combustion process and phasing effects with all three fuels and both EGR rates are presented here. Experimentally, the engine is operated at MBT CA50 combustion phasing until phasing retard is required to mitigate knock. The results, shown in Figure 5, illustrate that there are significant fuel-specific differences in both the KLSA (i.e., CA50 phasing) and EGR-antiknock effectiveness. For example, Figure 5 shows the combustion phasing of each fuel−EGR rate combination at three different speeds and how the fuels behave differently in the knock-limited regime.

Figure 5 shows that the trend in decreasing knock tendency with retarded combustion phasing is most prevalent with fuel E30. In other words, retarding combustion phasing is more effective at mitigating knock with E30 than with 87AKI or IB24. Interestingly, the knocking tendency of 87AKI and IB24 decrease sharply with increasing speed (less steep with increased speed). This trend is less pronounced with E30. Stein et al.[11] observed a similar reduced-knocking tendency with respect to engine speed with midlevel ethanol blends vs conventional distillates and low-level ethanol−distillate blends. They attributed this association to increased HoV of ethanol. The present study's results support their findings and also furthers the analysis with the addition of 15% EGR.

It is well known that EGR decreases knocking tendency. The present results illustrate with a 11.85 compression ratio, 87AKI+15% EGR remains more knock prone than IB24 or E30 with 0% EGR. For 87AKI and IB24 fuels, adding 15% EGR has a pronounced effect on reducing knocking tendency, similar to those previously reported by Alger et al.[19] In Alger's study, an approximate 0.5°CA less combustion retard is required per 1% external-cooled EGR. Their reported trends are supported in the present study's findings with 15% EGR and 87AKI gasoline. Based on this, approximately 24% and 32% external-cooled EGR, respectively, would be required to match the present study's antiknock properties with IB24 and E30 at 1200 r/min. Although that level of EGR is typical for diesel engines, this could be technically challenging in SI engines, even with high-energy ignition systems, because of the significantly decreased transient response, cylinder−EGR uniformity, flame kernel growth, and

dx.doi.org/10.1021/ef401575e | Energy Fuels XXXX, XXX, XXX−XXX

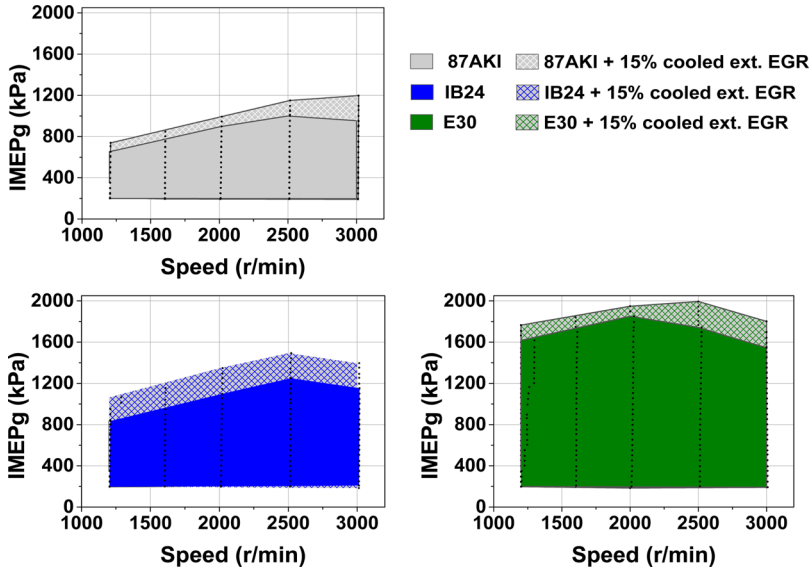

Figure 4. Gross load range of the tested fuels with and without EGR.

flame speeds with EGR. Based on the predicted amounts of EGR required to match the antiknock properties of E30, it is unlikely that EGR, with available market fuels, would be a feasible strategy for a large stoichiometric load expansion with a high compression ratio (i.e., high efficiency and power and torque density).

Conversely, with E30, adding 15% EGR offers less of an effect toward reducing knock. This is indicated by the nearly identical CA50 for a given load for E30 with and without EGR (~1°CA vs ≥2°CA advance for most conditions with EGR for the other fuels). This result demonstrates two phenomena are present. First, E30 exhibits a lower propensity to knock than the other fuels. Second, the increased knock protection provided by 15% EGR is minimal with E30. Therefore, with E30, EGR should be used primarily for reductions in thermal losses, pumping work, and emissions purposes than for knock mitigation. Interestingly, IB24 does not exhibit similar EGR trends to E30 with EGR, suggesting that molecular and chemical differences could be important with EGR effects on combustion. To explore whether combustion rate differences could be responsible for differences in KLSA and EGR phasing effects, a detailed combustion analysis is performed.

Combustion Duration Effects. It is well known that alcohol fuels have faster burning rates than petroleum distillates.[33,34] The present study supports these cited works. Figure 6 illustrates the combustion duration, defined as 5−90% mass fraction burned (MFB) time in °CA. Data are plotted as a function of IMEPg at a constant 2000 r/min speed at two EGR conditions. Although Figure 6 shows results for only one engine speed, similar trends are observed at all tested speeds. Note that as a function of IMEPg, the nonknock limited 5−90% MFB combustion durations are similar (i.e., IMEPg < 500 kPa). However, at IMEPg above 500 kPa, the trends diverge as each fuel encounters knock.

The results in Figure 6 demonstrate that for a given CA50 phasing, the knock-limited combustion durations are ordered as 87AKI > IB24 > E30. With both 87AKI and IB24 fuels, combustion duration increases as combustion phasing is retarded. This trend is either less pronounced or nonexistent with E30. The findings suggest two effects could be present with E30. First, under knocking conditions, E30 could reduce the end gas knock propensity because of the reduced time−temperature interactions and, thus, could further expand the load-range beyond that indicated by the RON or MON tests. Second, the faster combustion rate with E30 might enable higher EGR amounts than gasoline. Faster combustion aids in maintaining combustion stability as dilution or combustion phasing retard are increased because both effects tend to quench combustion rates. Additionally, the faster combustion with E30 might have important implications for ignition systems, as higher levels of EGR can require higher spark energy inputs and durations to decrease combustion duration.[21] However, it is unclear whether the combustion duration effects in Figure 6 are functions of the fuels or load.

To better understand the relations between combustion duration, load, and combustion phasing, a more detailed analysis is performed. First, combustion data of all fuels is compared under nonknock-limited operation. Figure 7 illustrates the cylinder pressure and HRR of each fuel at 2000 r/min 4 bar $IMEP_g$ load with MBT CA50 phasing of 8°CA after top dead center (ATDC) (i.e., no fuels knock limited).

The results illustrate that the initial portion of combustion is faster with the alcohol blends than with regular gasoline, where the 0−50% MFB rate of combustion is ordered as E30 > IB24 > 87AKI. However, after CA50, the fuels all have similar combustion characteristics. On the basis of the results, it is suggested that under nonknocking conditions, the later portions of combustion are less fuel-specific than the early portions of combustion. The present findings support previous combustion analysis work by Broustail et al.,[33] which has shown ethanol/isooctane and *n*-butanol/isooctane mixtures to have faster laminar burning velocities than isooctane. Although that work used *n*-butanol/isooctane mixtures, research by Liu et al.[35] has demonstrated that isobutanol and *n*-butanol have comparable flame speeds.

Although the present engine study complements cited fundamental combustion vessel studies, it remains unclear whether the faster MFB trends under KLSA are an effect of higher loads at which knock-limited operation occurs at (i.e., higher energy release) or a function of the fuels themselves. To isolate the effect of phasing independent of load, E30 is operated at the KLSA of 87AKI and IB24, with both 0 and 15% EGR.

dx.doi.org/10.1021/ef401575e | *Energy Fuels* XXXX, XXX, XXX−XXX

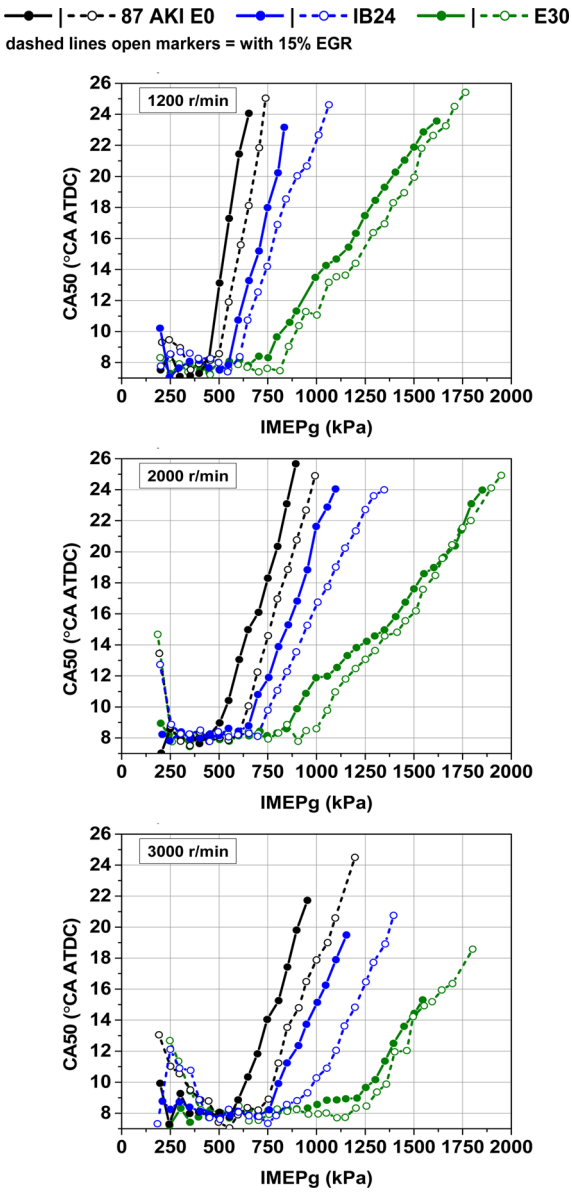

Figure 5. Combustion phasing for all fuels and EGR levels at (a) 1200 r/min, (b) 2000 r/min, and (c) 3000 r/min.

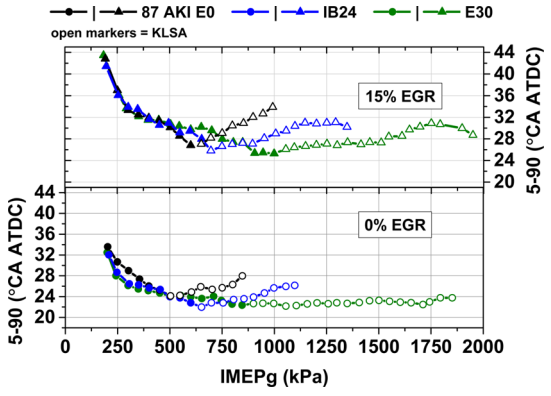

Figure 6. Combustion duration as defined by 5−90°CA for all tested fuels and EGR levels at 2000 r/min as a function of all IMEPg (left) and as CA50 after knock in the knock-limited regime (right).

Because end gas knock affects the later portions of combustion under KLSA operation, differences in combustion duration are

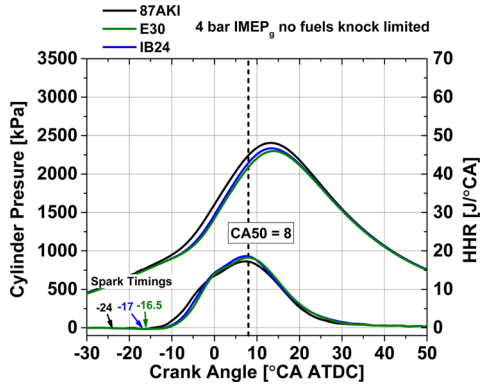

Figure 7. Indicated cylinder pressure and HRR of each fuel at 2000 r/min 4 bar IMEPg, CA50 of 8°CA ATDC.

expected. Figure 8 illustrates the combustion behavior for IB24 and 87AKI at their respective knock-limited phasing conditions, with CA50 phasing of 13°CA ATDC (loads of 600 kPa for 87AKI and 800 kPa for IB24) shown respectively at 2000 r/min.

Figure 8 shows that E30 retains a faster initial combustion duration (onset to CA50), but the knock-limited fuels have a faster second half of combustion. The faster second-half of combustion is likely caused by a small amount of end gas knock shortening the late combustion process. The presence of end gas knock is believed to be an effect of the method of defining knock-limited operation in the present study. Thus, at matched CA50 combustion phasing, the ensemble average traces of KLSA operation incorporate a small degree of end gas knock, expediting late stage combustion. Based on this definition of KLSA, it is most useful to compare the first and second half of the combustion separately (i.e., spark−5%, 5−50%, and 50−90% MFB). When compared in this manner, differences in combustion process of the alcohol/gasoline blends are most apparent.

The spark−5% MFB time represents the spark kernel growth time, the 5−50% MFB time represents the first half of combustion, and the 50−90% MFB time represents the late stage of combustion (when end gas knock can occur). The results for each fuel and both EGR rates at 2000 r/min are presented in Figure 9. Note that the dotted lines with green open triangles represent E30 operated at KLSA of 87AKI or IB24. The higher load E30 points have been truncated to retain higher resolution of the image at lower loads.

Figure 9 displays several key trends. First, without EGR (left figure), the spark−5% and 5−50% MFB times of 87AKI are slower than the intermediate alcohol−gasoline blend fuels. (This is qualitatively indicated in Figures 7 and 8 but is quantified in Figure 9). Second, with 0% EGR, the 50−90% MFB times are similar between fuels, with weak load dependence. However, when E30 is operated at later phasing (i.e., prematurely retarded to KLSA CA50 timing of 87AKI or IB24), the 5−50% MFB time remains significantly faster than the KLSA fuels, particularly compared to 87AKI. This indicates that, at least with 0% EGR, fuel composition has a large effect on the first half of the combustion process independent of phasing.

At 15% EGR operation (right figure), the fuel-specific effects are attenuated and CA50 combustion phasing dominates combustion duration. For example, operation of E30+15% EGR at the KLSA CA50 of 87AKI+15% EGR and IB24+15% EGR results in almost identical 5−50% MFB times at the respective CA50. Additionally, with 15% EGR, the spark−5% MFB and 5−50%

dx.doi.org/10.1021/ef401575e | *Energy Fuels* XXXX, XXX, XXX−XXX

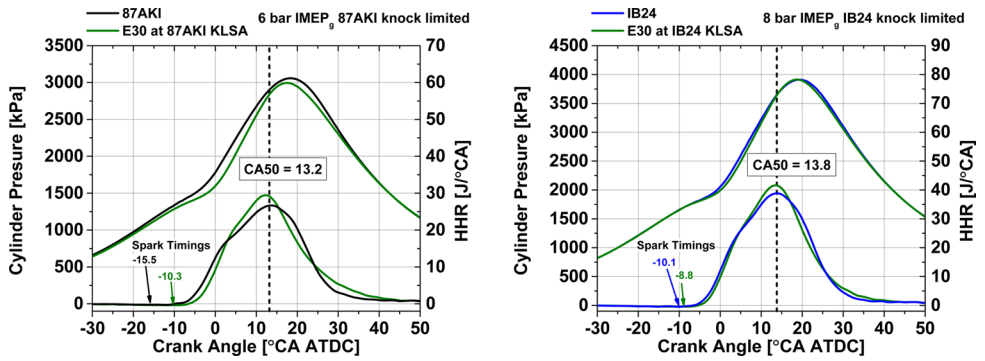

Figure 8. E30 (green) operated at KLSA of 87AKI at 6 bar IMEP$_g$ (left) and IB24 at 8 bar IMEP$_g$ (right).

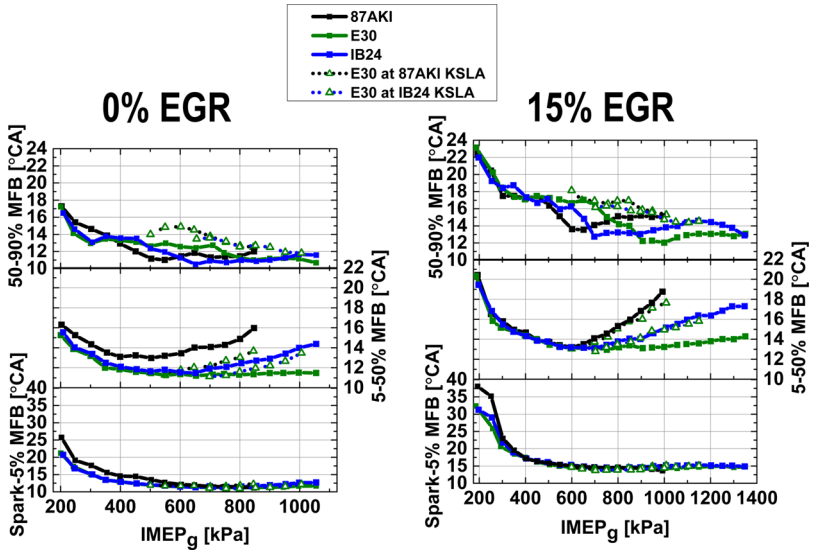

Figure 9. Heat release times of each fuel at 2000 r/min, with 0% EGR (left) and 15% EGR (right). Dashed line with open triangles are E30 prematurely retarded to at KLSA CA50 phasing of 87AKI of IB24, E30, and IB24 data truncated.

MFB times of each fuel is nearly identical. This result differs from the trends observed with 0% EGR, where 87AKI is slower. These results show that 15% EGR is more dominant at slowing down the early combustion stages more than intermediate alcohol−gasoline blends can increase the early stage combustion rate. A marked difference is seen with the alcohol−gasoline fuels at the lowest loads, with decreased spark−5% MFB times. On the basis of the trends observed with 0 and 15% EGR, it appears that fuel properties have a stronger effect with 0% EGR than with 15% EGR. To further explore these effects, only the KLSA portion of each fuel is compared in Figure 10 (i.e., different loads but matched CA50 times). Note that E30 at KLSA of 87AKI or IB24 (dotted lines and open green triangles) is E30 operated at both matched load and CA50 phasing to KLSA 87AKI or IB24.

Figure 10 illustrates that the spark−5% MFB times are similar for all fuels. However, fuel-specific differences exist for the 5−50% MFB duration with 0% EGR. Specifically, the 5−50% MFB duration is faster for E30 than either IB24 or 87AKI (left figure center). Note that the 5−50% MFB times are independent of load as E30 at KLSA of IB24 and that 87AKI (dashed lines and open triangles) are at lower loads than E30 KLSA but matched phasing to IB24 or 87AKI KLSA. Thus, this research suggests that fuel properties affect the first half of combustion with 0% EGR.

However, when 15% EGR is added, Figure 10 shows that combustion rate of all fuels slows. Interestingly, with 15% EGR the 5−50% MBF time of IB24 and E30 slow more than 87AKI, resulting in the 5−50% of all fuels being nearly identical (right figure center). Therefore, fuel effects are attenuated when EGR is added and phasing dominates combustion duration (i.e., turbulence and quenching). The trends in Figure 10 confirm that the trends of Figure 9 are the result of phasing and not load effects.

Similar to the 5−50% MFB trends, fuel-specific differences persist during the 50−90% MFB duration. For instance, the 50−90% MFB times of E30 at KLSA of 87AKI or IB24 (dashed lines in Figures 9 and 10) are longer in duration than 87AKI or IB24 at their matched phasing and load conditions. However, unlike the load independent trends of the 5−50% MFB times, Figures 9 and 10 illustrate that the 50−90% MFB times are highly dependent on load. This is highlighted by the longer combustion duration of E30 at the CA50 KLSA of 87AKI and IB24. Particularly, note that 87AKI is KLSA limited at a lower load, and E30 at 87AKI CA50 KLSA phasing exhibits the longest 50−90% MFB time followed by E30 at IB24 CA50 KLSA. This result demonstrates that the later portions of combustion are dominated by chemical or fuel-specific effects, specifically end gas knock, which is load dependent. Interestingly, with 15% EGR (right figure) the 50−90% MFB times are more spread out and ordered by 87AKI > IB24 > E30, suggesting that with 15% EGR, load might have an increasing importance on the late stage burning rate.

This analysis shows that with 0% EGR, E30 provides a chemical effect that shortens the initial stages of combustion,

dx.doi.org/10.1021/ef401575e | *Energy Fuels* XXXX, XXX, XXX−XXX

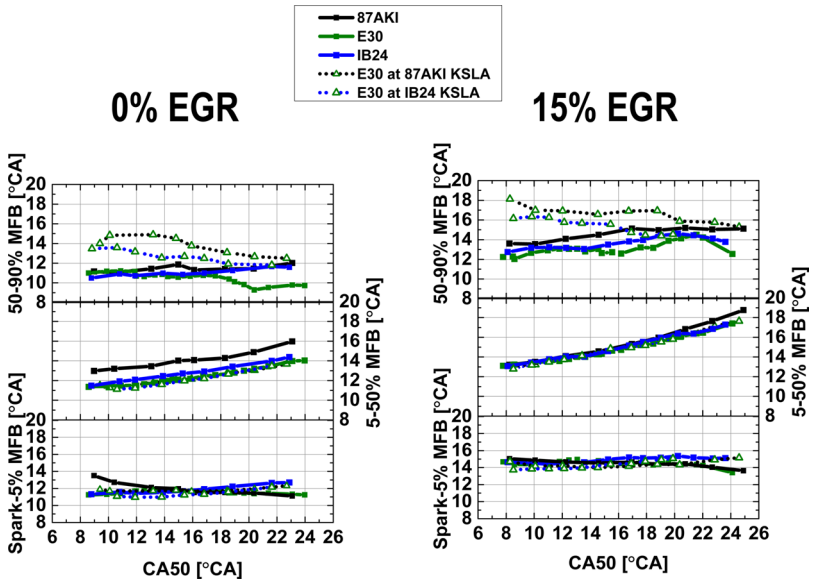

Figure 10. Flame kernel growth, 5−50%, and 50−90% MFB durations for each fuel, including matched CA50 combustion phasing and load to KLSA 87AKI and IB24 operation (dashed lines, open triangles) with 0% EGR (left) and 15% EGR (right).

providing shorter total combustion duration as well as a higher initial knock resistance. These findings have important implications, as faster combustion duration is important for reducing end gas knock propensity and increasing engine efficiency. Faster combustion reduces the time−temperature history of the end gas, which is well known to correlate with knock.[25] Additionally, faster combustion enables increased work extraction by increasing the expansion volume after combustion. Likewise, this increase in work extraction also reduces exhaust gas temperature (EGT), which can be beneficial to increasing the island of $\lambda = 1$ operation before catalyst protection with full time or part-time fuel enrichment[36] or other means of thermal protection is required.[37] For these purposes, there has been significant effort in the SI engine research and development communities to shorten combustion duration.[38] The present results show that there could be added advantages to decreasing combustion duration with midlevel alcohol−gasoline blends such as E30.

Thermal Efficiency Effects. The previous section analyzed the combustion phasing and duration effects. The data and corresponding analysis show that intermediate alcohol−gasoline blends offer particular combustion rate and antiknock advantages that might be more favorable for engine efficiency and load expansion. This section presents a first-law thermodynamic analysis of the fuel energy budget and estimates the adiabatic flame temperature of the fuels.

Figure 11 shows the gross thermal efficiency (GTE) for 2000 r/min operation with each fuel, with and without EGR. Regardless of fuel type or EGR rate, the trend is the same: GTE initially increases with load, reaches a maximum, and then decreases. For each fuel, the decrease in GTE while approaching the high load limit is due to combustion phasing retard for knock mitigation. The primary reason that E30 can achieve higher peak efficiency than 87AKI is that it can operate to higher loads without encountering knock-limited phasing.

Although the fuel-specific differences are most apparent at the high loads in Figure 11, there are also efficiency differences that are observed at light load with 0% EGR. At MBT combustion phasing (<600 kPa IMEPg) IB24 and E30 show a minor advantage in GTE relative to 87AKI. These findings are in

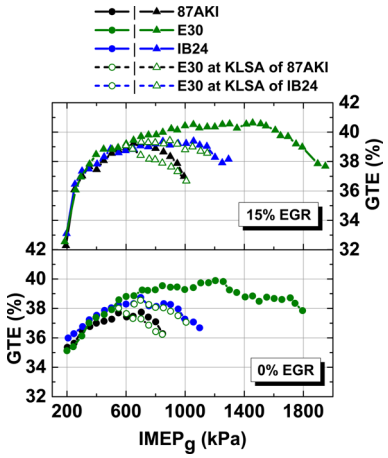

Figure 11. Gross thermal efficiency of each fuel at 2000 r/min operation with 0% EGR (lower) and 15% EGR (upper). Note that E30 is also operated at matched KLSA CA50 phasing of 87AKI and IB24 (indicated by open symbols).

agreement with Jung et al.[12] and Szybist et al.,[23,39] who both showed fundamental rationale for higher efficiencies with ethanol. The increase in GTE with 15% EGR is in agreement with Alger et al.[19] and can be attributed to the thermodynamic benefits of EGR.

Figures 12 and 13 show the EGT and exhaust (EXH) loss trends, respectively. The EXH losses are determined using the approach described in Splitter et al.[40] by solving for the enthalpy of the exhaust and intake with the 9-order NASA thermodynamic curve fits[41] applied to air and the measured exhaust species concentrations. The dominant feature of these figures is that the EGT and EXH losses increase sharply as the high load limit for each fuel is approached. These increases are due to retarded combustion phasing, which is required to mitigate knock. The retarded combustion phasing decreases the amount of expansion work that can be done; as a result, the increases EGT and EXH losses accompanied by decreases in GTE, as shown in Figure 11.

dx.doi.org/10.1021/ef401575e | *Energy Fuels* XXXX, XXX, XXX−XXX

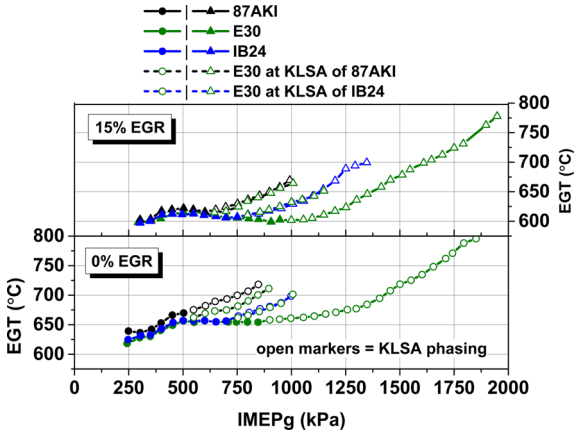

Figure 12. Exhaust gas temperature vs load for each fuel (0% EGR operation (lower), 15% EGR operation (upper)). Note that E30 is also operated at matched KLSA CA50 phasing of 87AKI and IB24 with and without EGR.

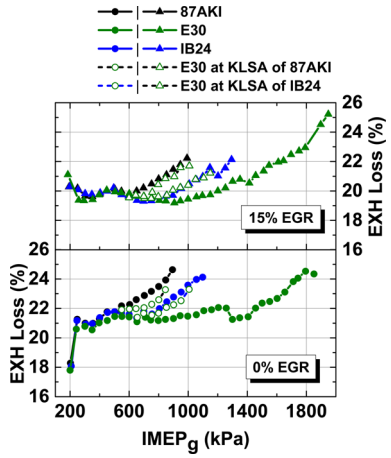

Figure 13. Exhaust loss vs load for each fuel (0% EGR operation (lower), 15% EGR operation (upper)). Note that E30 is also operated at matched KLSA CA50 phasing of 87AKI and IB24 with and without EGR.

Although the high load trends are the dominant features in Figures 12 and 13, the EGT and associated EXH losses are slightly lower for IB24 and E30 than for 87AKI with 0% EGR at matched MBT loads (loads less than 500 kPa IMEPg). This trend does not extend to the 15% EGR condition. Thus, the observed increase in GTE at the low load conditions in Figure 11 with 0% EGR operation of E30 and IB24 is at least partly attributed to reduced EGT and EXH losses, where EGR affects the EGT and EXH losses. The reason why EGT and EXH losses are lower for E30 and IB24 with 0% EGR is further explored by calculating the representative adiabatic flame temperature (TF_{aid}).

TF_{aid} is calculated for each fuel and EGR rate at a representative experimental condition with 52 °C intake temperature and $\lambda = 1$. The calculation approach assumes that the start of combustion and all loads are equal between the fuels and EGR rates, with an assumed peak combustion pressure of 7500 kPa (i.e., high load). To calculate TF_{aid}, the enthalpy of the products and reactants are set equal, with the product temperature determined by iterative solving. The reactant temperature is determined from assuming ideal gas behavior in eq 2, using the γ as calculated from the experimental composition. (The γ is determined from the slope of the compression stroke through the log of pressure−volume of experimental data.)

$$\frac{T_{\text{reactants}}}{T_{\text{IVC}}} = \frac{V_{\text{IVC}}}{V_{\text{reactants}}}^{(\gamma-1)} \quad (2)$$

Determining the reactant temperature using eq 2 enables the HoV to be bounded and demonstrates the range that TF_{aid} can be influenced by fuel HoV. The bounding of HoV uses two assumptions: the first is to ignore fuel HoV completely and assume that T_{IVC} in eq 2 is the same as the intake temperature (52 °C). The second is to assume that the entire fuel HoV instantly cools the in-cylinder reactants at intake valve close (i.e., starting reactant temperature (T_{IVC}) < 52 °C).

In addition to fuel HoV effects, dissociation effects are also determined. For either HoV assumption, dissociation effects are calculated by determining the product state through minimization of Gibbs free energy. The approach follows the discussion presented in Turns[42] using equilibrium analysis inclusive of CO_2, H_2O, N_2, O, OH, H, H_2, CO, NO, and NO_2. Less than 0.2% error with respect to full chemical equilibrium can be achieved using only these species (error less than 5K at the modeled conditions). The calculation results are presented in Figure 14, with 0% EGR in the lower plot and 15% EGR in the upper plot.

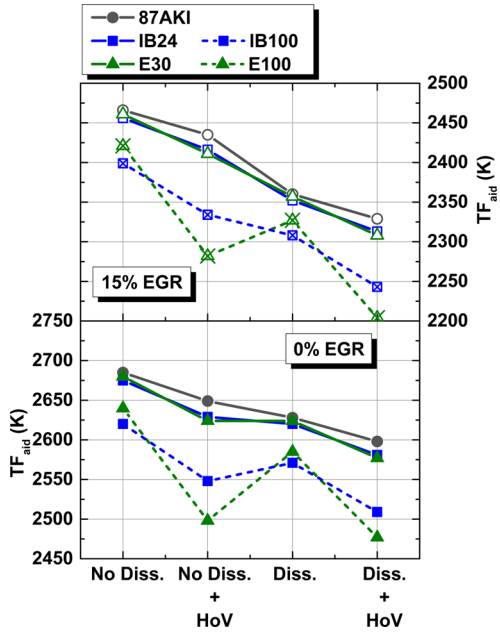

Figure 14. Adiabatic flame temperatures of $\lambda = 1$ operation of the three fuels and neat isobutanol and ethanol, all with and without EGR, with different assumptions (same scaling).

Figure 14 shows that for each HoV and dissociation assumption, the TF_{aid} of IB24 and E30 are slightly lower than gasoline (on the order of 20K lower when HoV is accounted for), which can have implications on heat transfer throughout the cycle. These findings are additionally supported in work by Jung et al.[12] This figure also illustrates the role of EGR on TF_{aid}. First, EGR is a diluent, and at 15%, it has the effect of reducing TF_{aid} by more than 200K when dissociation is not accounted for. However, because of higher concentrations of CO_2 and H_2O are present with EGR use, there is additional chemical dissociation. As a result, there is a larger reduction in TF_{aid} from dissociation when EGR is present. To better observe and isolate the effects

dx.doi.org/10.1021/ef401575e | Energy Fuels XXXX, XXX, XXX−XXX

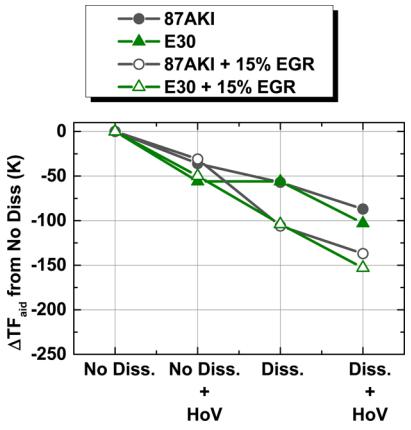

Figure 15. Change in TF_{aid} vs ideal for E30 and 87AKI.

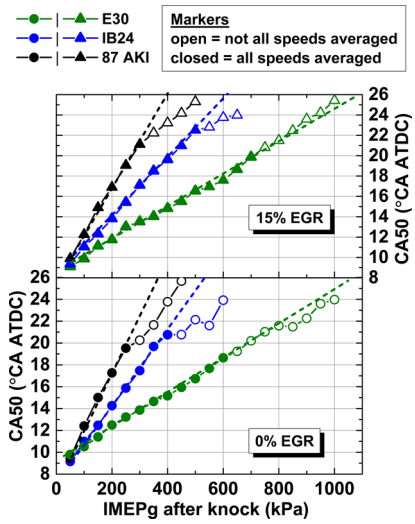

Figure 16. Average knock-limited phasing by fuel and EGR. Results are obtained by averaging as many speeds as possible. (All speeds averaged conditions are noted with filled markers, and fewer than all speeds averaged are noted with the open markers).

of HoV and dissociation when EGR is used, Figure 15 compares the difference in TF_{aid} relative to the baseline condition for 87AKI and E30. Note that both 0 and 15% EGR are plotted on a common axis in this figure and that trends are relative. It is noteworthy that the TF_{aid} reduction associated with the chemical dissociation is a more dominant effect than the fuel chemistry. Thus, though minor differences in TF_{aid} do exist between fuels, there is substantially more authority to affect TF_{aid} with EGR than with fuel composition. This is thought the be a contributing reason for why the EGT and EXH losses of 87AKI IB24 and E30 are most similar when 15% EGR was used; specifically, the chemical advantage of the intermediate alcohol−gasoline fuels on work increases and heat transfer reductions were reduced.

Fuel Octane Number Sensitivity. The octane number sensitivity of the fuels are ordered as 87AKI > IB24 > E30. The octane number sensitivity (S) of a fuel is defined as the RON-MON. As pointed out by Leppard,[43] S is a measure of the extent to which a fuel differs from alkane fuels. The octane number scale is based on *n*-heptane and isooctane, alkanes, in which by definition S is defined to be 0. Leppard[43] indicated that this S convention results in the S of normal and isoalkanes to be very low. More recently, Mittal et al.[44] used computational simulations to show this effect with biofuels, which included a 96 RON ethanol−alkane blend. Their results suggested that the low-temperature chemistry reactions are inhibited with ethanol but that the high temperature reactions are faster. Their findings support the present study's observed faster combustion durations with E30. The cited studies demonstrate the importance of the S of a fuel. It is well known that the antiknock properties of alkanes are highly speed and conditionally dependent. Therefore, by the octane index convention adopted, a fuel with a high S value is actually less conditionally dependent than a fuel with a low S value.[25,43,44] With this perspective, the observed power and torque-speed range trends in Figure 5 becomes more apparent.

To better compare the knock-limited regimes of each fuel−EGR combination, the KLSA CA50 as a function of IMEPg after knock was investigated. The IMEPg after knock is the load obtained after entering the knock limited regime, in which a value of 0 IMEPg denotes the knock limit. The results from the analysis are presented in Figure 16. For each fuel and EGR combination, the knock-limited combustion phasing of all speeds are averaged. However, because the operational constants of combustion phasing and EGT are reached under knock limited operation, the knock limited range of each speed is different. In Figure 16, different markers are used to denote this difference in the number of speeds used in speed averaging. A solid marker is used when all five engine speeds are averaged, and an open marker is used when fewer than all speeds are averaged. (Fewer than all 5 speeds are averaged at some loads because of either CA50 or EGT constraint being met by at least one speed.) Also, an "all speeds averaged conditions" linearity line is added for reference.

Each fuel displays a strong linear trend when all speeds are averaged (solid markers). However, once fewer speeds can be averaged (as indicated by the open data markers), the trends in 87AKI and IB24 deviate, exhibiting more speed sensitivity. The speed sensitivity of 87AKI and IB24 compared with E30 may be caused by both chemical phenomena associated with slower combustion duration and a difference in the octane sensitivity, S, of the each fuel.

From the CA50 as a function of knock-limited load comparison in Figure 16, it is clear that 87AKI and IB24 are more speed sensitive than E30. That is, the KLSA phasing of E30 remains linear (dashed line in Figure 16) for the open data markers, illustrating that the phasing retard for E30 is nearly independent of engine speed. Conversely, as engine speed decreases, more retard is required with 87AKI and IB24 to mitigate knock, pushing the open markers off from the linearity line. Additionally, with the 15% EGR, the effect of speed on phasing was even further reduced with E30, where almost no speed sensitivity was observed.

Knock-limited SI operation is similar to autoignition regimes like homogeneous charge compression ignition (HCCI), which use controlled autoignition as the combustion process. Therefore, it is useful to compare the results of previous HCCI studies to those of knock-limited SI combustion regimes. In an HCCI study by Sjöberg and Dec,[45] it was shown that gasoline and ethanol exhibit significantly different speed dependencies, which complements the previous computational work by Mittal et al.[44] For example, in boosted HCCI tests by Dec and Yang,[46] it was demonstrated that conventional E0 gasoline becomes more reactive (approaching *n*-heptane) at a fixed engine load-speed as intake pressures approach approximately 2 bar. A follow up study by Dec et al.[47] confirmed the pressure sensitivity E0 trends were also present with E10 fuel. Conversely, it was shown by Sjöberg and Dec[45] that, at the same conditions, the reactivity of neat ethanol showed no pressure dependency. That study

dx.doi.org/10.1021/ef401575e | *Energy Fuels* XXXX, XXX, XXX−XXX

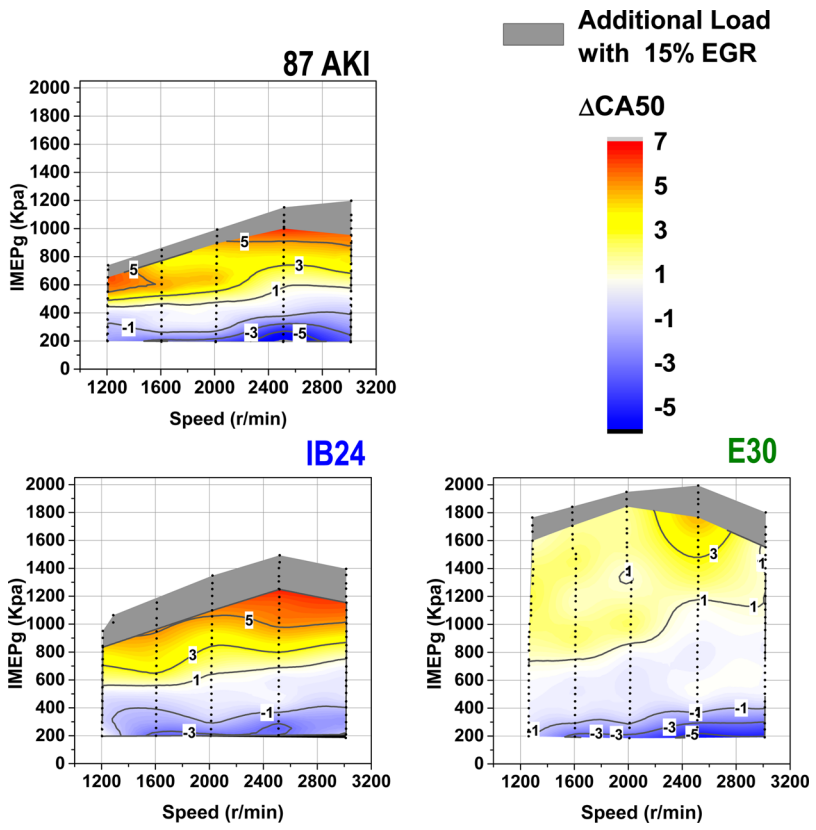

Figure 17. Contours of phasing difference (CA50) with 15% EGR for each respective fuel.

demonstrated that ethanol exhibited a very weak speed dependency, unlike alkane-based fuels. A numerical investigation by Mehl et al.[48] indicated that at the tested conditions, gasoline can enter pressure-sensitive low-temperature chemistry reactions, increasing the reactivity (reducing the effective octane number) of the fuel. Although the combinations of these studies are different in overall combustion process, the autoignition event in HCCI is similar to end gas knock in SI combustion. Therefore, the aforementioned HCCI study's findings are relevant to the present work in that the reactivity of ethanol has a less dependent ignition process with respect to pressure (i.e., 15% EGR) and speed conditions.

In SI combustion at $\lambda = 1$, in-cylinder pressure can be changed with load, compression ratio, EGR, camshaft phasing, and combustion duration effects (i.e., combustion phasing and burning rate). Because the present study operated the engine with fixed valve timing at MBT or KLSA phasing, the effects of combustion rates and phasing are minimal. Moreover, the compression ratio was fixed across the entire study; thus at a given load, EGR is the only parameter that can influence pressure history. EGR affects the ratio of specific heats (γ), the total pressure, and the pressures of O_2 and diluents (M body) while simultaneously reducing the temperature (a mass and γ effect). Thus, a direct quantification of the pressure effects of EGR is difficult. However, the trends of Figures 6−11 show that EGR is important in knock mitigation for 87AKI and IB24 but less so for E30. To better illustrate the differences, the CA50 of operation with 15% EGR was subtracted from the CA50 with 0% EGR. This ΔCA50 is shown in the contour plots of Figure 17.

The results illustrate that regardless of engine speed and load, the effect of 15% EGR with E30 is small (on the order of 1°CA of phasing advance relative to 0% EGR). However, the other fuels show an increasing CA50 phasing advantage at higher loads, with over a 5°CA of CA50 phasing advance relative to 0% EGR. As mentioned, the reasons for this are not entirely clear in the present study. This conditional EGR CA50 phasing dependency with 87AKI and IB24 could be the result of the increased pressure with 15% EGR at $\lambda = 1$ operation, effectively increasing the reactivity of 87AKI and IB24 more than that of E30, and therefore counteracting some of the antiknock benefits of EGR. However, the present study does show that by adding 15% EGR, the knocking tendency of E30 is similar regardless of speed. Because EGR reduces the temperature history of the engine, the lack of speed dependence with E30 suggests that thermal ignition could be more temperature dependent with E30 than the other fuels. This is supported by the neat ethanol HCCI findings of Sjöberg and Dec,[45] in which temperature was found to be the dominant influence on ethanol HCCI control more than pressure. Their finding has implications on the nature and size of knock-limited operation with E30. That is, E30 enables higher loads at lower engine speeds without knock and without EGR.

With E30, the relative lack of knock resistance provided by EGR is small and the knock resistance provided by the fuel is large. This affords the opportunity of E30 to increase the engine's stoichiometric torque capability at a high compression ratio more than the other tested fuels without being EGR dependent at high boost and low engine speeds (where simultaneously generating boost and driving EGR is more challenging for turbomachinery). This inherent benefit with E30 could enable practical increases in engine power densities with less complicated air-handling systems. Furthermore, the combustion duration and speed sensitivity findings suggest that high *S* high RON fuels may be more optimal for highly boosted downsized engines.

dx.doi.org/10.1021/ef401575e | *Energy Fuels* XXXX, XXX, XXX−XXX

DISCUSSION

The present study demonstrates that improvements to the base engine design and efficiency might be enabled by midlevel alcohol−gasoline blends, like IB24 and E30. Specifically, E30 displays improved antiknock tendencies beyond the values defined by the RON and MON tests. Additionally, E30 was found to be more tolerant to EGR than the other fuels, with short combustion durations maintained under knock-limited conditions. The results demonstrate that the use of midlevel alcohol blends, such as E30, enables additional engine downsizing with the potential for $\lambda = 1$ operation. This is addressed in greater detail in the companion paper to the present study (part 1).[32] However, the engine's stoichiometric torque capability at high compression ratio can be doubled with E30 fueling as compared to 87AKI gasoline. The focus on engine efficiency for this study dictated the choice of a compression ratio of approximately 2 points higher than stock (11.85:1 vs 9.2:1), biasing the results toward higher octane fuels. However, if high engine efficiency is required to meet imposed CAFE standards in conjunction with the RFS II standards, then higher efficiency engines will be required. Improvements to engine efficiency made possible with ethanol fuels may be a synergistic approach to simultaneous compliance with CAFE and RFS II. This presents a unique and infrequent opportunity to dramatically alter internal combustion engine operation by improving fuel properties.

CONCLUSIONS

The findings of this study are applicable to SI engine fuel economy and performance. Specifically, two midlevel alcohol blends, E30 and IB24, are compared to regular pump gasoline (87AKI) with 0% ethanol. The fuels are compared with 0 and 15% EGR at five speeds from 2 bar IMEPg to a full-load condition, where either a combustion phasing or an EGT limit is met. The results demonstrate that E30 with 15% EGR offers the highest stoichiometric torque capability at a high compression ratio.

A detailed combustion analysis is performed with each fuel−EGR rate combination. The analysis demonstrates that E30 and IB24 offers faster spark−50% MFB times, whereas 50−90% MFB times are dominated by knock and load. Interestingly, 15% EGR is found to offer less of an advantage at mitigating knock with E30 than the other tested fuels. Furthermore, E30 is observed to have little speed dependency and fast combustion durations in the knock-limited regime. These properties enable an expansion of the knock-limited regime to a wider load and speed range, with a smaller efficiency penalty in the knock-limited regime.

The combined findings demonstrate that midlevel ethanol blends offer more than high RON, MON, and HoV values, in that they can exhibit improved combustion and knock mitigation phenomena, especially with midlevel ethanol blends like E30. Changes to the fuel infrastructure through midlevel alcohol blends could be enabling steps for feasible near-term increases in vehicle efficiency and reductions in CO_2.

AUTHOR INFORMATION

Corresponding Author

*E-mail: splitterda@ornl.gov.

Notes

Disclosure: This paper has been authored by a contractor of the U.S. Government under contract number DE-AC05-00OR22725. Accordingly, the U.S. Government retains a nonexclusive, royalty-free license to publish or reproduce the published form of this contribution, or allow others to do so, for the U.S. Government.

The authors declare no competing financial interest.

†E-mail: szybistjp@ornl.gov.

ACKNOWLEDGMENTS

The authors gratefully acknowledge the support of the U.S. Department of Energy, particularly Kevin Stork and Steve Przesmitzki of the Vehicle Technologies Office. Additionally, the authors would like to acknowledge Vicki Kalaskar for assistance with the engine test laboratory.

ABBREVIATIONS

EPA, U.S. Environmental Protection Agency; RFS II, Renewable Fuels Standard II; CAFE, corporate average fuel economy; SI, spark ignition; LD, light-duty; NOx, oxides of nitrogen; CO, carbon monoxide; HC, hydrocarbon; CH4, methane; HoV, enthalpy of vaporization; MPG, miles per gallon; EGR, exhaust gas recirculation; λ, lambda; γ, ratio of specific heats; HVA, hydraulic valve actuation; CA, crank angle; AFR, air fuel ratio; $ATDC_{fi}$, after top dead-center firing; ATDC, after top dead center; $IMEP_g$, indicating mean effective pressure gross; RON, research octane number; MON, motor octane number; LHV, lower heating value; ASTM, American Society of Testing and Materials; TF_{aid}, adiabatic flame temperature; GTE, gross thermal efficiency; HRR, heat release rate; KLSA, knock-limited spark advance; MFB, mass fraction burned; *S*, sensitivity; CA50, crank angle at 50% mass fraction burned; AKI, antiknock index; E30, 30% ethanol and gasoline by volume; E0, 0% ethanol by volume; IB24, 24% isobutanol and gasoline by volume; FID, flame ionization detector; HCCI, homogeneous charge compression ignition

REFERENCES

(1) One Hundred Tenth Congress of the United States of America, Energy Independence and Security Act of 2007. 2007; H.R. 6.

(2) U.S. Environmental Protection Agency, "40 CFR Part 80 Regulation of Fuels and Fuel Additives: 2011 Renewable Fuel Standards; Final Rule". www.gpo.gov/fdsys/pkg/FR-2010-12-09/pdf/2010-30296.pdf (accessed May 2, 2013).

(3) Energy information agency transportation sector energy consumption report. www.eia.gov/totalenergy/data/monthly/#consumption (accessed May 2, 2013).

(4) National Highway Traffic Safety Administration and Environmental Protection Agency, "2017 and Later Model Year Light-Duty Vehicle Greenhouse Gas Emissions and Corporate Average Fuel Economy Standards; Final Rule," www.nhtsa.gov/fuel-economy (accessed May 2, 2013).

(5) U.S. Environmental Protection Agency, "Light-Duty Automotive Technology, Carbon Dioxide Emissions, and Fuel Economy Trends: 1975 Through 2012," www.epa.gov/fueleconomy/fetrends/1975-2012/420r13001.pdf (accessed May 2, 2013).

(6) Fraser, N.; Blaxill, H.; Lumsden, G.; Bassett, M. Challenges for Increased Efficiency through Gasoline Engine Downsizing. *SAE Int. J. Engines* **2009**, *2* (1), 991−1008, DOI: 10.4271/2009-01-1053.

(7) Stein, R.; Polovina, D.; Roth, K.; Foster, M. Effect of Heat of Vaporization, Chemical Octane, and Sensitivity on Knock Limit for Ethanol - Gasoline Blends. *SAE Int. J. Fuels Lubr.* **2012**, *5* (2), 823−843, DOI: 10.4271/2012-01-1277.

(8) Stein, R.; House, C.; Leone, T. Optimal Use of E85 in a Turbocharged Direct Injection Engine. *SAE Int. J. Fuels Lubr.* **2009**, *2* (1), 670−682, DOI: 10.4271/2009-01-1490.

(9) Szybist, J.; Foster, M.; Moore, W.; Confer, K.; et al. Investigation of Knock Limited Compression Ratio of Ethanol Gasoline Blends. *SAE Technical Paper* **2010**, 2010−01−0619, DOI: 10.4271/2010-01-0619.

(10) Szybist, J. P.; Chakravathy, K.; Daw, C. S. Analysis of the Impact of Selected Fuel Thermochemical Properties on Internal Combustion

Engine Efficiency. *Energy Fuels* **2012**, *26* (5), 2798−2810, DOI: 10.1021/ef2019879.
(11) Stein, R.; Anderson, J.; and Wallington, T. An Overview of the Effects of Ethanol−gasoline Blends on SI Engine Performance, Fuel Efficiency, and Emissions. *SAE Int. J. Engines* **2013**, *6*(1), doi: 10.4271/2013-01-1635
(12) Jung, H.; Shelby, M.; Newman, C.; and Stein, R. Effect of Ethanol on Part Load Thermal Efficiency and CO2 Emissions of SI Engines. *SAE Int. J. Engines* **2013**, *6*(1), doi: 10.4271/2013-01-1634.
(13) Jung, H.; Leone, T.; Shelby, M.; Anderson, J. et al. Fuel Economy and CO2 Emissions of Ethanol−gasoline Blends in a Turbocharged DI Engine. *SAE Int. J. Engines* **2013**, *6*(1), doi: 10.4271/2013-01-1321.
(14) Szybist, J.; West, B. The Impact of Low Octane Hydrocarbon Blending Streams on the Knock Limit of "E85". *SAE Int. J. Fuels Lubr.* **2013**, *6* (1), 44−54, DOI: 10.4271/2013-01-0888.
(15) Anderson, J. E.; Kramer, U.; Mueller, S. A.; Wallington, T. J. Octane Numbers of Ethanol − and Methanol − Gasoline Blends Estimated from Molar Concentrations. *Energy Fuels* **2010**, *24* (12), 6576−6585, DOI: 4134154/ef101125c.
(16) Anderson, J.; Leone, T.; Shelby, M.; Wallington, T., et al. ″Octane Numbers of Ethanol−gasoline Blends: Measurements and Novel Estimation Method from Molar Composition,″ *SAE Technical Paper 2012-01-1274*, **2012**, 10.4271/2012-01-1274.
(17) Foong, T. M.; Morganti, K. J.; Brear, M. J.; da Silva, G.; Yang, Y.; Dryer, F. L. The octane numbers of ethanol blended with gasoline and its surrogates. *Fuel* **2014**, *115*, 727−739.
(18) High Octane Fuel Symposium, International Society of Automotive Engineers, January 2013, Washington, D.C., www.sae.org/events/hofs/.
(19) Alger, T.; Mangold, B.; Roberts, C.; Gingrich, J. The Interaction of Fuel Anti-Knock Index and Cooled EGR on Engine Performance and Efficiency. *SAE Int. J. Engines* **2012**, *5* (3), 1229−1241, DOI: 10.4271/2012-01-1149.
(20) Wheeler, J.; Polovina, D.; Ramanathan, S.; Roth, K.; et al. Increasing EGR Tolerance using High Tumble in a Modern GTDI Engine for Improved Low-Speed Performance,″. *SAE Technical Paper 2013-01-1123* **2013**, DOI: 10.4271/2013-01-1123.
(21) Alger, T.; Gingrich, J.; Mangold, B.; Roberts, C. A Continuous Discharge Ignition System for EGR Limit Extension in SI Engines. *SAE Int. J. Engines* **2011**, *4* (1), 677−692, DOI: 10.4271/2011-01-0661.
(22) Splitter, D. A.; Szybist, J. P. Intermediate Alcohol-Gasoline Blends. Fuels for Enabling Increased Engine Efficiency and Powertrain Possibilities. Technical Paper 2014-01-1231, 2014, accepted for publication; DOI: 10.4271/2014-01-1231.
(23) Szybist, J.; Nafziger, E.; Weall, A. Load Expansion of Stoichiometric HCCI Using Spark Assist and Hydraulic Valve Actuation. *SAE Int. J. Engines* **2010**, *3* (2), 244−258, DOI: 10.4271/2010-01-2172.
(24) Weall, A.; Szybist, J.; Edwards, K.; Foster, M.; et al. HCCI Load Expansion Opportunities Using a Fully Variable HVA Research Engine to Guide Development of a Production Intent Cam-Based VVA Engine: The Low Load Limit. *SAE Int. J. Engines* **2012**, *5* (3), 1149−1162, DOI: 10.4271/2012-01-1134.
(25) Heywood, J. B. *Internal Combustion Engine Fundamentals*, McGraw-Hill: New York, 1988.
(26) Federal Register, vol *75*(213), Thursday, November 4, 2010, Notices.
(27) Federal Register, vol *76*(17), Wednesday, January 26, 2011, Notices.
(28) US Environmental Protection Agency proposed ruling, "Control of Air Pollution from Motor Vehicles: Tier 3 Motor Vehicle Emission and Fuel Standards". www.epa.gov/otaq/tier3.htm (accessed May 2, 2013).
(29) National Renewable Energy Laboratory Report, "Utilization of Renewable Oxygenates as Gasoline Blending Components". www.nrel.gov/docs/fy11osti/50791.pdf (accessed May 2, 2013).
(30) American Petroleum Institute, Alcohols and Ethers, A Technical Assessment for Their Application as Fuels and Fuel Components, 3rd ed., *API Pub. 4261*, June 2001.
(31) Wilhoit, R. C.; Zwolinski, B. J. *Physical and Thermodynamic Properties of Aliphatic Alcohols Journal of Physical and Chemical Reference Data*, 1973, *2*, Supplement No. 1.
(32) Splitter, D. A.; Szybist, J. P. An Experimental Investigation of Spark Ignited Combustion With High Octane Bio-Fuels and EGR. 1. Engine load Range and Downsize Downspeed Opportunity. *Energy Fuels* **2014**, DOI: 10.1021/ef401574p.
(33) Broustail, G.; et al. Experimental determination of laminar burning velocity for butanol and ethanol iso-octane blends. *Fuel* **2011**, *90*, 1−6.
(34) Verhelst, S.; Vancoillie, J.; Demuynck, J. A correlation for the laminar burning velocity for use in hydrogen spark ignition engine simulation. *Int. J. Hydrogen Energy* **2011**, *36* (1), 957−974.
(35) Liu, Wei; Kelley, A. P.; Law, C. K. Non-premixed ignition, laminar flame propagation, and mechanism reduction of< *n*-butanol, isobutanol, and methyl butanoate. *Proc. Combust. Inst.* **2011**, *33* (1), 995−1002.
(36) Nose, H.; Inoue, T.; Katagiri, S.; Sakai, A.; et al. Fuel Enrichment Control System by Catalyst Temperature Estimation to Enable Frequent Stoichiometric Operation at High Engine Speed/Load Condition. *SAE Technical Paper* **2013**, 2013−01−0341, DOI: 10.4271/2013-01-0341.
(37) Grandin, B.; Ångström, H. Replacing Fuel Enrichment in a Turbo Charged SI Engine: Lean Burn or Cooled EGR. *SAE Technical Paper 1999, 1999-01-3505* **1999**, No. 10.4271/1999-01-3505.
(38) Mattavi, J. The Attributes of Fast Burning Rates in Engines. *SAE Technical Paper* **1980**, 800920 DOI: 10.4271/800920.
(39) Szybist, J. P.; Chakravathy, K.; Daw, C. S. Analysis of the impact of selected fuel thermochemical properties on internal combustion engine efficiency. *Energy Fuels* **2012**, *26* (5), 2798−2810.
(40) Splitter, D.; Wissink, M.; DelVescovo, D.; Reitz, R. RCCI Engine Operation Towards 60% Thermal Efficiency. *SAE Technical Paper 2013-01-0279* **2013**, DOI: 10.4271/2013-01-0279.
(41) McBride, B. J.; Zehe, M. J.; and Gordon S. NASA Glenn coefficients for calculating thermodynamic properties of individual species. *National Aeronautics and Space Administration, John H. Glenn Research Center at Lewis Field*, 2002.
(42) Turns, S. R. *An introduction to combustion*; McGraw-Hill: New York, 1996; Vol. *499*.
(43) Leppard, W. The Chemical Origin of Fuel Octane Sensitivity. *SAE Technical Paper* **1990**, 902137 DOI: 10.4271/902137.
(44) Mittal, V.; Heywood, J.; Green, W. The Underlying Physics and Chemistry behind Fuel Sensitivity. *SAE Int. J. Fuels Lubr.* **2010**, *3* (1), 256−265, DOI: 10.4271/2010-01-0617.
(45) Sjöberg, M.; Dec, J. Ethanol Autoignition Characteristics and HCCI Performance for Wide Ranges of Engine Speed, Load and Boost. *SAE Int. J. Engines* **2010**, *3* (1), 84−106, DOI: 10.4271/2010-01-033.
(46) Dec, J.; Yang, Y. Boosted HCCI for High Power without Engine Knock and with Ultra-Low NOx Emissions - using Conventional Gasoline. *SAE Int. J. Engines* **2010**, *3* (1), 750−767, DOI: doi:10.4271/2010-01-1086.
(47) Dec, J.; Yang, Y.; Dronniou, N. Improving Efficiency and Using E10 for Higher Loads in Boosted HCCI Engines. *SAE Int. J. Engines* **2012**, *5* (3), 1009−1032, DOI: 10.4271/2012-01-1107.
(48) Mehl, M.; Pitz, W.; Sarathy, M.; Yang, Y.; et al. Detailed Kinetic Modeling of Conventional Gasoline at Highly Boosted Conditions and the Associated Intermediate Temperature Heat Release. *SAE Technical Paper 2012-01-1109*, 2012, 10.4271/2012-01-1109.